Dissertations
Department of Chemistry
University of Eastern Finland

No. 135 (2016)

Linlin Sun

The Effects of Structural and Environmental Factors on the Swelling Behavior of Montmorillonite-Beidellite Smectites: a Molecular Dynamics Approach

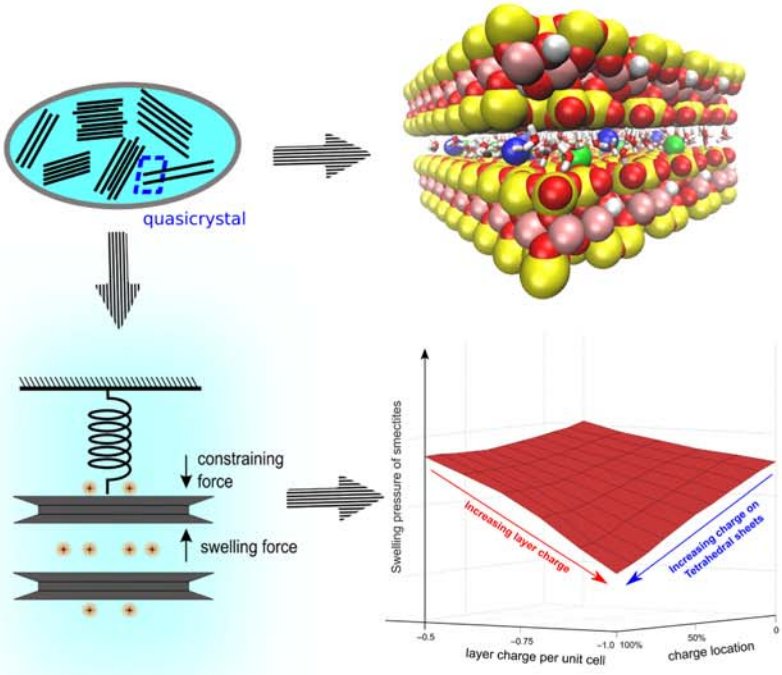

The Effects of Structural and Environmental Factors on the Swelling Behavior of Montmorillonite-Beidellite Smectites: a Molecular Dynamics Approach

Linlin Sun

Department of Chemistry
University of Eastern Finland
Finland

Joensuu 2016

Linlin Sun

Department of Chemistry, University of Eastern Finland

P.O.Box 111, FI80101 Joensuu, Finland

Supervisor

Prof. Tapani Pakkanen, University of Eastern Finland, Joensuu, Finland

Referees

Prof. Jukka Lehto, University of Helsinki, Helsinki, Finland

Prof. Maarit Karppinen, Aalto University, Espoo, Finland

Opponent

Prof. Markus Olin, VTT Technical Research Center of Finland LTD, Espoo, Finland

To be presented with the permission of the Faculty of the Science and Forestry of the University of Eastern Finland for public criticism in Auditorium F100, Yliopistokatu 7, Joensuu, on February 19th, 2016, at 12 o'clock noon.

ISBN: 978-952-61-2045-4 (print)

ISSNL: 1798-5668

ISSN: 1798-5668

ISBN: 978-952-61-2046-1 (PDF)

ISSN: 1798-5676 (PDF)

Grano Oy Jyväskylä

Joensuu 2016

Abstract

Smectites are lamellar clay minerals that readily swell in the presence of water. The swelling properties of smectites play a key role in many engineering applications, including environmental remediation, catalysis, and geological disposal of nuclear waste. The swelling behavior of smectite containing clays are regulated by multiple structural and environmental factors. The structural factors include the composition of clays, the interlayer cation species, the total layer charge, the substitution type and substitution distributions, whereas the environmental factors includes temperature, pressure and the salinity of the surrounding solutions. In this study, molecular dynamics simulation is employed to investigate the cross-effects of these structural and environmental factors on swelling characteristics and, in particular, the swelling pressure of the montmorillonite-beidellite smectite series.

The influence of interlayer cation compositions in couple with temperature and pressure were investigated with a periodical montmorillonite model. The simulations of Na-, Ca-, and Na/Ca mixed clays demonstrate that the swelling behaviour corresponding to each cation compositions are generally similar, but differ significantly in the transition range from 1- to 2-layer hydrate. This difference originates from the behaviour of interlayer calcium ions, which are found to promote the association of water molecules in their vicinity. This leads to uneven water distribution in the interlayer space and larger *d*-spacing in calcium dominant clays compared to that of sodium dominant clays.

Swelling pressure was also successfully modeled to account for the swelling behaviour of smectites with the use of molecular dynamics simulations. For Na-smectites with layer charges of –0.5 to –1.0e per unit cell, the swelling pressure was found to inversely correlate with the layer charge. Montmorillonite-like clays bearing dominant octahedral substitutions have a higher swelling pressure than beidellite-like clays that bear dominant tetrahedral substitutions. In contrast to Na-smectites where substantial swelling pressure is developed after intial hydration, Ca-smectites structures that differ in layer charge and charge location are exclusively found to lose their swelling pressure quickly as clay expands. The swelling pressure modeling also examines the influence of surrounding solutions. This is accomplished by immersing a montmorillonite structure into contact with pure water, sodium chloride and calcium chloride solutions. The swelling pressure was found to be lower in saline solutions than that in pure water, while calcium chloride solution caused more evident decreases in the swelling pressure than that of sodium chloride solutions. The modeled swelling pressure and its correlation to the compaction of clay were found to be in agreement with experimental data.

This study provides valuable atomic level information on the swelling behavior of smectites. A prediction for swelling pressure based on an atomic level computational approach is proposed and justified. This approach can potentially be used for the screening of swelling clays for various environmental and industrial applications.

List of Original Publications

This dissertation is a summary of publications I-II and a submitted manuscript III.

I. Sun, L., Tanskanen, J. T., Hirvi, J. T., Kasa, S., Schatz, T., Pakkanen, T. A. Molecular dynamics study of montmorillonite crystalline swelling: Roles of interlayer cation species and water content. *Chem. Phys.* **2015**, *455*, 23–31.

II. Sun, L., Hirvi, J. T., Schatz, T., Kasa, S., Pakkanen, T. A. Estimation of Montmorillonite Swelling Pressure: a Molecular Dynamics Approach. *J. Phys Chem. C* **2015**, *119*, 19863–19868.

III. Sun, L., Ling, C. Y., Lavikainen, L. P., Hirvi, J. T., Kasa, S., Pakkanen, T. A. Influence of layer charge and charge location on the swelling pressure of dioctahedral smectites. **2016***, submitted for publication.*

The applicant had an essential role in designing the modeling approach used in all the articles **I – III**. The applicant carried out all modeling work and data analysis in articles **I – II**, and a major part of the simulation work in article **III**. The applicant had the main responsibility for writing all the articles **I – III**. The co-authors contributed in commenting on the writing.

Contents

Abbreviations

1W	1-layer hydrate
2W	2-layer hydrate
3W	3-layer hydrate
$CaCl_2$	Calcium Chloride
HLRW	High level radioactive waste
MD	Molecular dynamics
NaCl	Sodium Chloride
NPT	Isothermal-isobaric ensemble
NVT	Canonical ensemble
SPC	Simple Point Charge
O	Octahedral
T	Tetrahedral

1. Introduction

1.1 Clays and clay minerals

Clays and clay minerals are naturally occurring or synthetic materials composed primarily of fine-grained minerals, which are generally plastic at appropriate water contents and will harden when dried or fired.[1] They are not only the material of many kinds of ceramics, but also an essential constituent of plastics, paints, paper, rubber, and cosmetics.[2] The diversity of clay structures and properties, and their wide-ranging applications has driven intensive research into clay for decades.

In terms of numerous environmental and industrial uses, smectites are among one of the most important clays.[2,3] The rock in which smectites are dominant is bentonite.[4] Bentonite is conventionally used in iron ore pelletizing, foundry mouldings, oil-well drilling, filtering, clarifying, decoloring, as adsorbents for toxins, and sanitary landfill (**Figure 1a**).[2,5-7] In recent years, the properties of smectites have been intensively investigated, with the result that many new uses have been developed.[8-19] Major developments aim to use bentonite, mostly smectites, as catalysts and catalyst supports, [8-14] and other applications in pharmaceuticals[15,16] and in the production of clay polymer nanocomposites.[17] In particular, bentonite and bentonite-aggregate mixtures have been chosen as buffer and backfill materials in the future construction of geological repositories for high level radioactive waste (HLRW)[18,19] (**Figure 1b**). As an important part of the multiple release barriers, bentonite is expected to separate the radioactive waste from the surroundings for an extended time of e.g. 10,000 or even 100,000 years.[20]

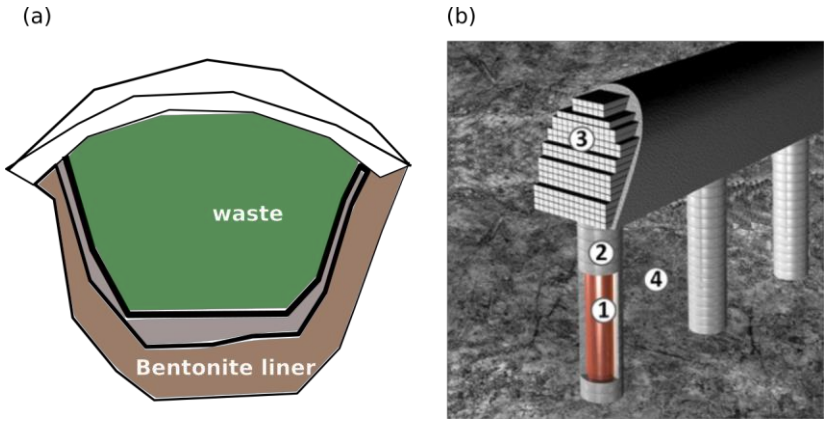

Figure 1. (a) The use of bentonite clay in sanitary landfill. (b) Multiple release barriers in the nuclear waste final disposal system: ① final disposal canister, ② bentonite buffer, ③ tunnel backfill (containing bentonite), ④ bedrock. Figure 1b obtained from ref 21.

1.2 The structure of smectites

Smectites are organized in quasicrystals. Quasicrystals are sets of 2:1 phyllosilicate layers in parallel. Each quasicrystal consists of between two to thousands of individual layers stacked together, whereas the individual layer consists of an octahedral (O) sheet sandwiched between two tetrahedral (T) sheets (**Figure 2**). Isomorphous replacements with lower-valency metal ions, Mg^{2+} and Fe^{2+} substituting Al^{3+} in the O sheet, and Al^{3+} substituting Si^{4+} in the T sheets, give the structure a total negative charge. For smectites, the layer charge typically ranges from –0.4 to –1.2e per unit cell. The negative charge is balanced by the interlayer cations stoichiometrically; Na^{+}, K^{+}, Ca^{2+} and Mg^{2+} are the most commonly interlayer cation species in natural occurring smectites.[22]

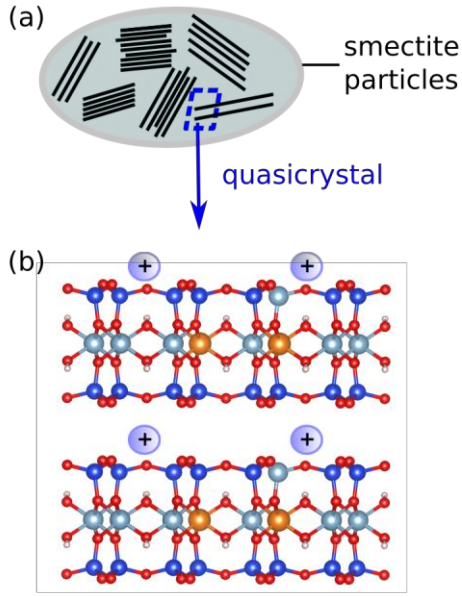

Figure 2. (a) Smectite particles and (b) the layer structure. The color code of the atoms is blue for silicon, cyan for aluminum, orange for magnesium, red for oxygen and white for hydrogen. The positive sign represents the interlayer cations.

The types of smectites are distinguished by the variations in their chemical structures. Generally, smectites can be classified according to the following criteria: i) dioctahedral or trioctahedral structure, ii) predominant octahedral and tetrahedral substitutions, iii) layer charge and charge location. The most important dioctahedral and trioctahedral end-members of smectites and their idealized formulas are listed in **Table 1**. Montmorillonites allocate the layer charge mostly in the O sheet, while beidellite allocates the majority of the layer charge in the T sheets. Just for the montmorillonite-beidellite smectite series, Emmerich et al. proposed that 96 structural

variables theoretically exist based on several structural varibles including the layer charge and charge location.[23]

Table 1. Idealized formula of some representative smectites

Type	Names	Idealized formula per unit cell
Dioctahedral	Montmorillonite	$[Al_{4-y}Mg_y]\ [Si_8]\ O_{20}(OH)_4$
	Beidellite	$[Al_4]\ [Si_{8-x}Al_x]\ O_{20}(OH)_4$
	Nontronite	$[Fe_4]\ [Si_{8-x}Al_x]\ O_{20}(OH)_4$
	Valkonskoite	$[Cr_4]\ [Si_{8-x}Al_x]\ O_{20}(OH)_4$
Trioctahedral	Hectorite	$[Mg_{6-y}Li_y]\ [Si_8]\ O_{20}(OH)_4$
	Saponite	$[Mg_6]\ [Si_{8-x}Al_x]\ O_{20}(OH)_4$
	Sauconite	$[Zn_6]\ [Si_{8-x}Al_x]\ O_{20}(OH)_4$

1.3 The swelling property of smectites

In the presence of water, smectites readily swell. The swelling ability is key to the many uses of smectites as it affects the movement of aqueous solutions and the transportation of chemical elements.[24] As one of the most important properties of smectites, the swelling process is regulated by multiple structural and environmental factors.[25-37] To establish how the clay swelling depends on these factors, the joint effects of these factors should be systematically evaluated.

With respect to the structural factors, the interlayer cation compositions, the layer charge and the charge location are of particular importance. The species, size and charge of the exchangeable interlayer cations are known to impact on the swelling behavior.[28,30,38-40] The swelling of clays is positively correlated to the hydration energy of the monovalent interlayer cations, although cations with high charge are found to be strongly associated with negatively charged sites on the clay surfaces and cause less swelling.[30,31,41] The layer charge can also significantly influence the swelling behavior of clays.[25,35] Slade and Christidis suggest that a high layer charge causes limited swelling, while low charged smectites swell continuously.[25,42] However, there are also studies suggesting that swelling increases with an increasing layer charge due to the strong hydration of the interlayer cations.[35,43,44] The type and the location of the charges arising from isomorphous substitution also plays an important role in swelling.[45] Early studies suggest that *d*-spacings are larger in the presence of octahedral substitution in comparison to the clay structures with dominant tetrahedral substitutions.[34,46] Also, the interlayer cations tend to form inner-sphere complexes in the presence of tetrahedral substitutions and cause less swelling. For clays with mostly octahedral substitutions, the formation of outer-sphere cation-water complexes are preferred and cause increased swelling.[26,47,48]

Environmental factors, including temperature, pressure and the properties of the surrounding solutions, are also known to affect the swelling behavior of smectites.[35-37] The water retention and swelling capacity were found to decrease as temperature and pressure increases.[37]Also, with an increase in the salinity of the surrounding solutions, the swelling potential was found to reduce greatly.[25,49]

1.4 The swelling pressure of smectites

The swelling property and the generation of sufficient swelling pressure is of crucial importance for the use of smectites as an engineered barrier in HLRW disposal.[22,50] Upon swelling, smectite minerals in the bentonite buffer exert swelling pressure. In the context of HLRW disposal, the development of swelling pressure can result in the sealing of gaps and openings in the buffer and its contacts with the host rock and the waste canisters.[51,52] Sufficient swelling provides effective sealing, which is critical for: i) limiting the transport of dissolved agents that corrode the canister materials and potential HLRW releases from the canister, ii) protecting the canister from sinking and rock movements, and iii) reducing microbial activity. The understanding and the screening of swelling pressure for the candidate buffer material is therefore a key issue in consideration of the long term safety of HLRW geological disposal.

A clay structure with short interlayer spacing gives high dry density, which correlates to large swelling pressure.[53] The reported swelling pressure typically ranges from less than 1 MPa to even 60 MPa with respect to different smectite structures and the experimental conditions.[54] However, the complex physico-chemical nature of smectites has prevented the discovery of experimental techniques from measuring the swelling pressure of smectites without the complications of disorder, poor crystallinity, and mixed charge or hydration states in natural smectite samples.[55]

1.5 The Aims of this study

The study summarized in this dissertation aims at predicting the swelling characteristics and the swelling pressure of montmorillonite-beidellite smectites in the consideration of multiple variables. The specific objectives of this study were as follows:

(i) To understand the swelling characteristics with varying water content and interlayer cation compositions;
(ii) To obtain atomic level interactions among multiple structure components and the effects of temperature and pressure;
(iii) To model and to justify the model of swelling pressure based on an atomic-level computation approach;
(iv) To predict the swelling pressure of montmorillonite-beidellite smectites with respect to a variation of layer charges, charge locations, and interlayer cations;
(v) To investigate the swelling pressure in the salt solutions.

2 Computational aspects

Computational chemistry has gained great popularity in recent decades with the rapid improvement in computer technology. The technology can either be used for interpretation of experimental results or to shed light on the atomic or molecular interactions of chemical systems. Mostly importantly, it can also serve as a predictive tool for investigating physico-chemical properties for which experimental data are difficult to obtain or interpret. In this study, the computation models based on delineating the key forces and dynamics at atomic level provide a cost-effective way to simulate the complex interactions between the clays and their water environment.

The structure of the model system is shown in **Figure 3**. The model combines a water model and a clay mineral model into a molecular dynamics model. Molecular dynamics simulations were performed by using a Gromacs simulation package.[56] The parameterization for the interatomic potential energy terms was taken from a CLAYFF force field.[57] The visualization and analysis of MD simulation results were carried out by tools including Gaussview, VMD, Material Studio, and Chimera.

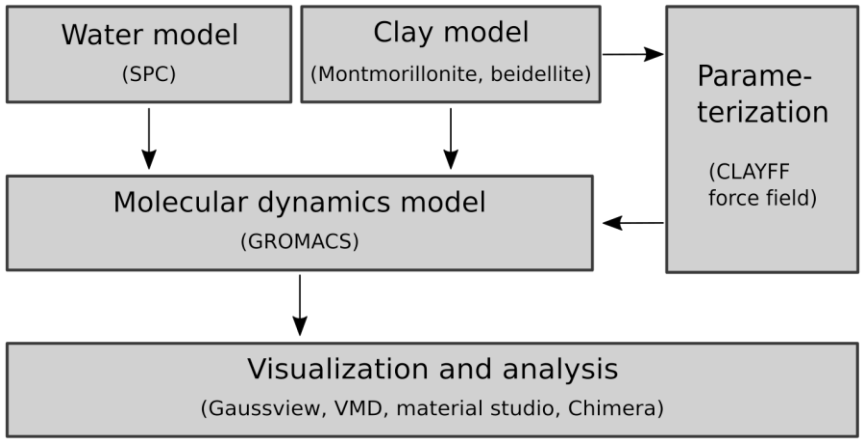

Figure 3. Structure of the model system used in this work.

2.1 Molecular dynamics simulations

Among the main modern modeling tools, molecular dynamics (MD) simulation has become a powerful technique for investigating the dynamic behavior of chemical systems.[58] The method was originally conceived within theoretical physics in the late 1950s, but is applied today mostly in chemical physics, materials science, and the modeling of biomolecules. MD enables simulation of the dynamics of a complex system using finite time steps, which calculate energy and forces between the particles using molecular mechanics force fields. With regard to clay modeling, MD allows bulk

simulations that are adjustable to include hundreds of thousands of atoms, and it mimics the interactions between clay and its surrounding salt solution at different scales. The MD approach is hereby employed to simulate the swelling behavior of smectites, and to further investigate the effects of structural and environmental factors on the swelling characteristics of smectites.

2.2 The CLAYFF force field

Successful application of MD simulations requires the use of interatomic potentials that effectively and accurately account for the interactions of all atoms in the investigated system. CLAYFF is a general force field suit for hydrated, multi-component mineral systems and their interfaces with aqueous solutions. Since clays are heterogeneous, partly unstructured, and of high molecular complexity, the CLAYFF approach treats most interatomic interactions as non-bonded. This allows the use of the force field for a wide variety of phases and properly accounts for energy and momentum transfer between the fluid phase and the solid phase.[57] The water molecules in the simulation system are parameterized by the most used water model (SPC),[59] which is sufficiently accurate and allows for the calculation of a large system with an affordable calculation time.

3 Crystalline swelling: roles of interlayer cation compositions and water content [I]

Experimental studies have revealed that the swelling of smectites exhibits two regimes: crystalline swelling and osmotic swelling.[45] Crystalline swelling occurs through the stepwise formation of a 1-layer hydrate (1W), 2-layer hydrate (2W) and 3-layer hydrate (3W). In crystalline swelling the *d*-spacing increases from about 1.0 nm in the dehydrated state up to about 1.9 nm, whereas in the osmotic swelling, the *d*-spacing increases continuously.[30]

There have been comprehensive experimental and theoretical studies conducted on Na- and Ca-smectites.[25,34,43,46,60,61] However, systems with multiple cation species have received less attention. The natural clay minerals, however, usually simultaneously contain more than one species of cations.[62] Hereby, we have investigated the swelling characteristics of montmorillonite clay with different interlayer cation compositions. Through our simulation work, the arrangement of interlayer species and their interactions with clay layers are studied. The influence of temperature and pressure on the hydrated structures of clay minerals are also explored.

3.1 System setup

A montmorillonite clay model with chemical composition of $(Si_{7.75}Al_{0.25})(Al_{3.5}Mg_{0.5})O_{20}(OH)_4$ is utilized in this work. The total layer charge is –0.75e per unit cell. The model includes two clay layers where each layer contains 4 × 4 unit cells (**Figure 4**). Interlayer cations with a total charge of +24e are incorporated into the system to balance the negative charged clay layers. Four simulation systems with different counterion compositions were considered: i) Na-montmorillonite with pure Na^+, ii) system Mixed I with 4:1 Na^+/Ca^{2+} ratio, iii) system Mixed II with 1:1 Na^+/Ca^{2+} ratio, iv) Ca-montmorillonite with pure Ca^{2+}. To mimic the swelling process, water molecules were added stepwise into the interlayers up to a water content of 0.4 g/g (grams of water per 1 g of clay). The cations and water molecules were placed randomly within the interlayer space.

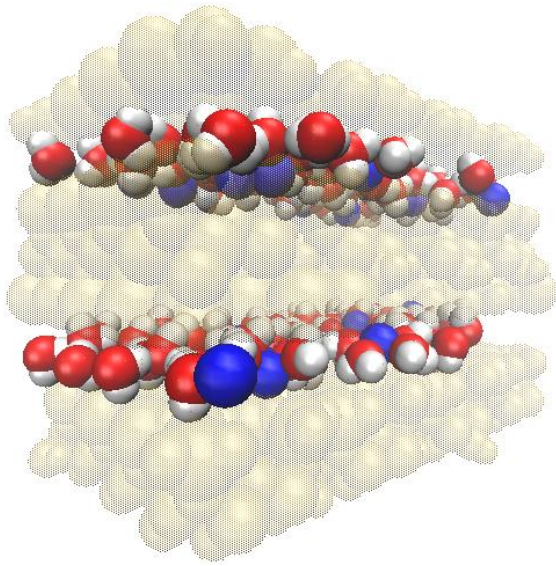

Figure 4. Model setups for Na-montmorillonite. The clay structure is represented in transparent yellow. The color code is red for oxygen, white for hydrogen and blue for interlayer Na^+ ions.

The swelling of montmorillonite with different cation compositions was first studied at baseline conditions of 300 K and 0.1 MPa. Simulations were also performed under different temperatures (260 K, 340 K, and 380 K), while keeping the pressure constant (0.1 MPa). In addition to the variations in temperature, the variations of pressures (4 MPa, 8 MPa, 12 MPa, and 16 MPa) were also considered while keeping the temperature constant (300 K). All simulations were carried out in an isobaric-isothermal (NPT) ensemble. The simulation systems were allowed to equilibrate for

200 ps, followed by a production run of 200 ps. Data were collected after every 0.025 ps throughout the production run.

3.2 Swelling of Na- and Ca-montmorillonites

The swelling curves at 300K and 0.1 MPa are shown in **Figure 5a**. The overall stepwise swelling in pure Na- and Ca-montmorillonite agrees well with previous simulations and experimental studies[57,63-65] (**Figure 5b and 5c**). Analogous to the swelling curves of pure Na- and Ca-montmorillonite, the swelling curves of the mixed Na/Ca-montmorillonites also show that the *d*-spacing increases non-linearly with increasing water content.

For both Na- and Ca-montmorillonite, the 1W and 2W states are identified on the basis of the location of the plateau in the swelling curves. The simulated *d*-spacings at corresponding layer hydrates are in line with the experimental results.[30,34,39,64,66-68] In particular, the simulated *d*-spacing for the 2W of Ca-montmorillonite in this work is closer to the *d*-spacing averaged from experimental studies than that of other theoretical studies.[30,34,66,69,70]

The four swelling curves significantly differ from each other at water content 0.05 to 0.15 g/g. Higher Ca^{2+} concentrations in the interlayer lead to larger *d*-spacings. At the first plateau that corresponds to 1W, the *d*-spacing for Ca-montmorillonite is about 0.05 nm larger than in Na-montmorillonite. Moreover, the first plateau around 1.2 nm *d*-spacing is less obvious for Ca-montmorillonite and the mixed systems compared to that of Na-montmorillonite. This suggests that the presence of Ca^{2+} ions alters the interactions and structural arrangements of the interlayer species at water contents from 0.05 - 0.15 g/g. The different *d*-spacing suggests the hydrate structure formed in Ca-montmorillonite differs from that in Na-montmorillonite. Hence, we have further analyzed the hydrate structures in the presence of Na^{+} and Ca^{2+} interlayer cations.

3.3 Atomic level structural arrangements and interactions in clay-water systems

The atomic density profiles from MD simulations at 1 atm and 0.1 MPa have demonstrated the formation of 1W, 2W and 3W for Na-montmorillonite at corresponding water contents (**Figure 6a-6d**). The density profile of water oxygen atoms at water contents of 0.07 and 0.11 g/g show a single peak corresponding to 1W. At a water content of 0.22 g/g, the density profile of water oxygen atoms has split into two peaks, symmetrical about the central cation peak, indicating the formation of 2W. The formation of 3W at a water content of 0.33 g/g is demonstrated by the three water oxygen peaks. Compared to Na-montmorillonite, the peak at a water content of 0.11 g/g becomes broader and shorter with an increasing concentration of Ca^{2+} in the interlayer space (**Figure 6e-6g**). For pure Ca-montmorillonite, a split peak is observed. The split indicates that in Ca-montmorillonite, the water molecules can reorganize and

start to form a 2W structure already at such a small water content. This finding agrees with the increasing *d*-spacing for Ca-containing montmorillonite, as shown **Figure 5**.

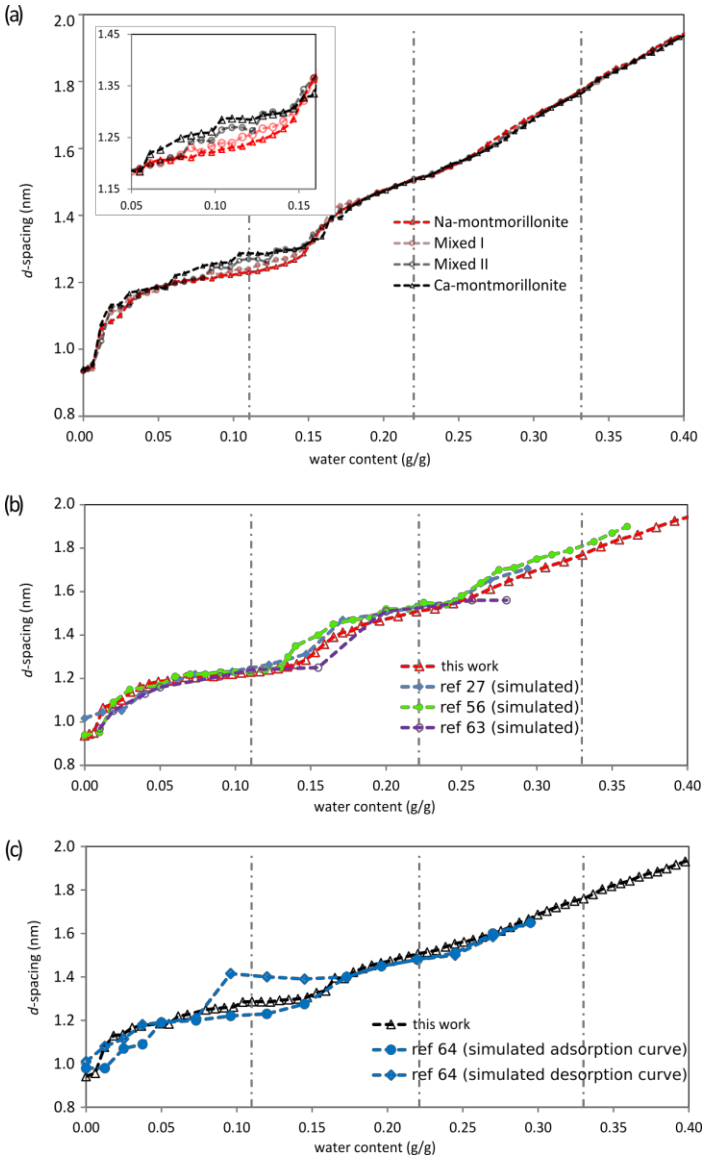

Figure 5. Swelling curves of (a) Na-montmorillonite, Ca-montmorillonite, and mixed Na/Ca-montmorillonites. The inset shows the details of the swelling curve at water contents from 0.05 – 0.15 g/g. Comparison of the simulated swelling curves of (b) Na-montmorillonite and (c) Ca-montmorillonite to other studies. The vertical lines indicate roughly the water contents of the 1W, 2W and 3W. The standard deviations of the simulated data are within the range of the symbols.

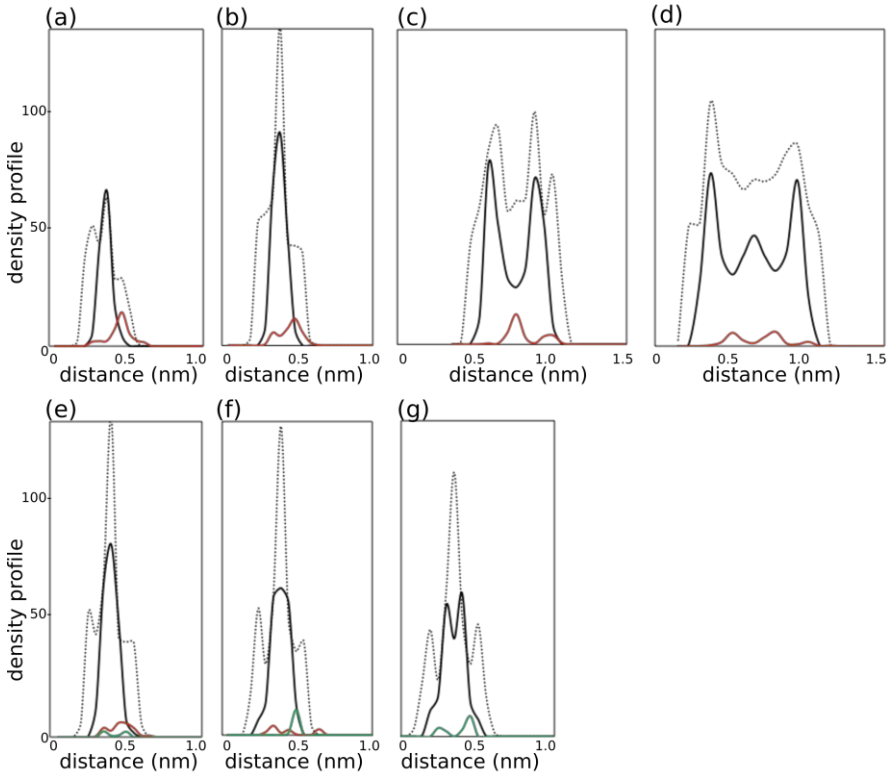

Figure 6. Number density profiles for interlayer species in Na-montmorillonite at water content of (a) 0.07, (b) 0.11, (c) 0.22, and (d) 0.33 g/g. The same density profiles are shown for (e) Mixed I, (f) Mixed II and (g) Ca-montmorillonite at water content 0.11g/g. The results for water oxygen atoms, water hydrogen atoms, Na^+ and Ca^{2+} are shown in solid black, dotted black, solid red, and solid green lines, respectively. The number density profiles are plotted relative to the distance to the center of the O sheet.

The clear differences between Na- and Ca-montmorillonite at low water contents are also confirmed by the molecular structures achieved from the equilibrium states of the simulations. **Figure 7** shows snapshots of hydrated structures of Na- and Ca-montmorillonite at a water content of 0.11 g/g. Water molecules in Na-montmorillonite are distributed between the clay basal surfaces with the first solvation shell of Na^+ highlighted. By contrast, in Ca-montmorillonite, the water molecules tend to interact primarily with Ca^{2+}. By taking a closer look at the cation coordination status, we find that half of the Ca^{2+} ions are coordinated to 5 water molecules; the rest of the Ca^{2+} ions form outer-sphere complexes that have a coordination number of 6. For Na-montmorillonite at the same water content, all Na^+ ions form inner-sphere complexes, coordinating to less than 4 water molecules. The outer-sphere complexes are bigger in

size that that of the inner-sphere complexes. In order to accommodate the larger Ca^{2+}-water outer-sphere complexes, expanded interlayer spacing is caused. This explains the differences in the swelling curves of montmorillonites with different Na^{+}/Ca^{2+} interlayer cation compositions.

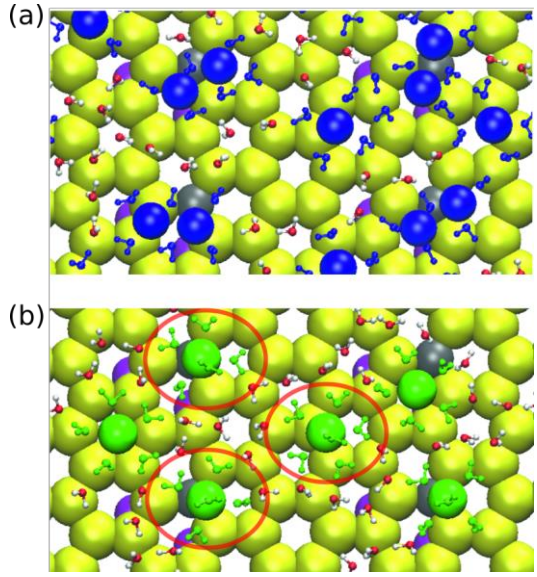

Figure 7. The final geometries for (a) Na-montmorillonite at water contents of 0.11 g/g, and for (b) Ca-montmorillonite at the same water content. Only the silicon atoms in the topmost T sheet and substitutions in T/O sheets are visualized for the clay. The color code of the atoms is yellow for silicon, grey for aluminum, purple for magnesium, red for oxygen, white for hydrogen, blue for sodium, and green for calcium. Water molecules residing in the first solvation shells have the same color as the corresponding cations. Red circles mark the Ca^{2+} ions coordinated to 6 water molecules, which form outer-sphere complexes.

3.4 The influence of temperature and pressure on interlayer structures

The simulated swelling curves at temperatures 260-380K also demonstrate a nonlinear increase of *d*-spacing as a function of water content. Due to the increased thermal motion of the interlayer species, increasing temperature results in increasing *d*-spacings. To clarify the effect of temperature, *d*-spacings of Na- and Ca-montmorillonite at temperatures of 260 K, 340 K, and 380 K are compared to the *d*-spacings at 300 K (**Figure 8a-8b**). In Na-montmorillonite, the temperature effect is marginal at low water contents but more pronounced at higher water contents. When in Ca-montmorillonite, variations can be seen throughout the whole water content range. Minor deviation occurs near water content 0.22 g/g, which corresponds to the formation of 2W.

The *d*-spacings at pressures of 4-16 MPa are compared to the *d*-spacings at 0.1 MPa (**Figure 8c-8d**). In general, the pressure is found to weakly influence the swelling of Na-montmorillonite for the investigated ranges. By contrast, the pressure causes great changes in *d*-spacings in Ca-montmorillonite prior to the formation of 2W. These changes in *d*-spacings are probably caused by the water migration between water molecules that organized at different water layers.

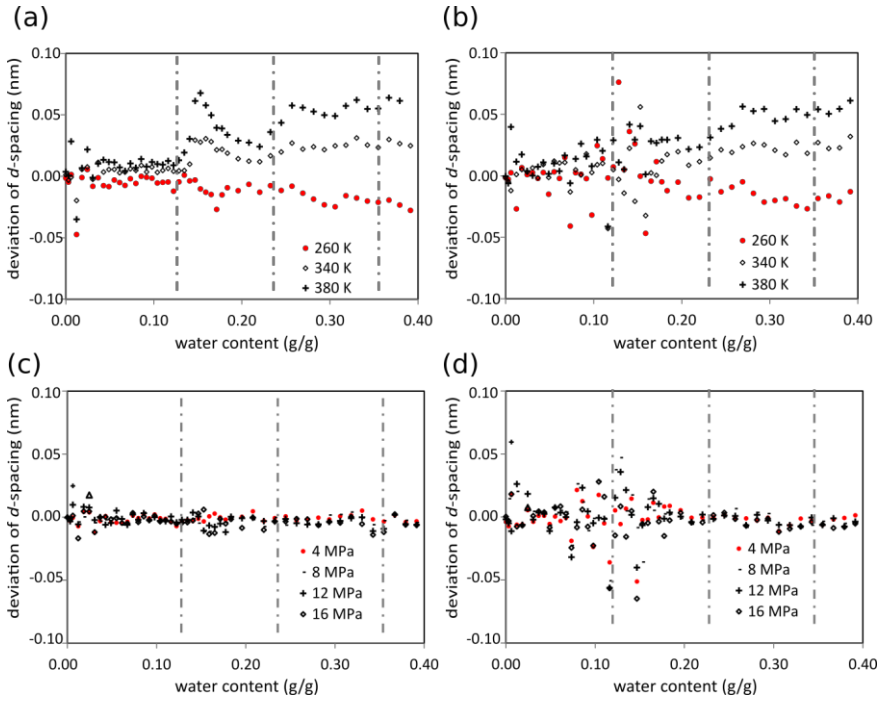

Figure 8. The influence of (a) temperature in Na-montmorillonite, (b) temperature in Ca-montmorillonite, (c) pressure in Na-montmorillonite, and (d) pressure in Ca-montmorillonite. The deviation in *d*-spacing is given relative to that at 300 K and 0.1 MPa. The vertical lines roughly indicate the water contents of the 1W, 2W and 3W.

The sensitivity of montmorillonite swelling seems to imply that for the studied ranges of temperature and pressure, the interlayer species in the forms of 1W and 2W in Na-montmorillonite as well as the 2W in Ca-montmorillonite are considerably stable. This agrees with the fact that the majority of the experimental studies reported the formation of 1W and 2W for Na-montmorillonite,[30,34,38,39,64,66,71-75] whereas the formation of the 3W was observed only in a few studies.[30,71,72,74] By contrast, most of the experimental studies have reported the formation of the 2W for Ca-montmorillonite,[30,34,66,67,69,70,76,77] whereas the formation of 1W and 3W was reported more rarely.[34,70] We hence hypothesized that 1W and 2W of Na-montmorillonite and the 2W of Ca-montmorillonite are more stable under the prevailing analysis conditions, allowing easier detection.

4 Swelling pressure modeling [II,III]

Swelling pressure has been studied intensively with experimental methods.[22,53,78,79] Theoretical models that predict swelling pressure are not seen from molecular simulations. In this work, a method to predict the swelling pressure of the swelling clays based on MD simulations has been developed and justified. The technique has enabled us to study the effects of both structural and environmental variables on the swelling pressure. The simulated swelling pressures are compared to experimental results whenever applicable. In general, the rather small and simple molecular dynamics model reproduces surprisingly well the montmorillonite swelling trends in water and salt solutions.

4.1 Spring model development

The scheme of the spring model for probing the swelling pressure in the clay-water system is presented in **Figure 9**. In this model, the quasicrystals of smectites are simplified as two clay layers. It is known that swelling and swelling pressure relies on water exchange between environmental bulk solution and water within quasicrystals or interlayers. Hereby, the two clay layers were put into contact with the bulk water solution. The lower smectite layer is held rigid throughout simulations, while the upper layer was allowed to move only in a vertical direction. At an initial configuration, a mechanical spring at equilibrium was attached to the upper clay layer. The spring has a force constant and follows Hooke's law. As swelling expansion occurs, the displacement in the vertical direction of the clay layer from its original position results in a compression of the spring from its relaxed (equilibrium) position and an increasing (restoring) spring force which serves to restrain the movement of the upper layer. In this process, the change in the spring length is equivalent to the change in the *d*-spacing. When the swelling reaches an equilibrium state, the force on the spring is assumed to be equal to the force of swelling. As such, the swelling forces and subsequently the swelling pressure can be calculated from the deformation of the spring.

The dependency of swelling pressure on the swelling states of clays is investigated by a series of simulations combining different spring constants and initial *d*-spacings. The magnitude of swelling is limited to *d*-spacings that depend on the value of the spring constant: the larger the spring constant, the less swelling is allowed. On the other hand, the initial *d*-spacing also varies from 1.4 to 3.0 nm. By adjusting the initial *d*-spacing and spring constant, we are expecting to simulate a wide range of swelling pressures as a function of *d*-spacing with high computational efficiency.

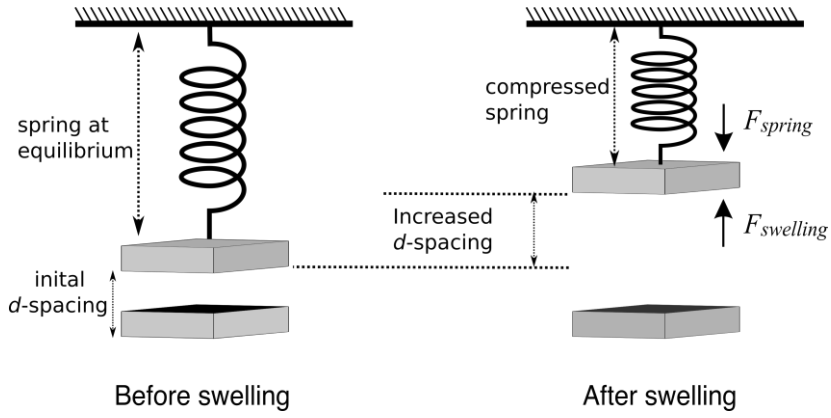

Figure 9. An illustration of the spring model. The bottom layer was fixed while the upper layer was allowed to move in a vertical direction. The spring force is compensated by a swelling force.

4.2 System setup

The simulation setup includes two clay layers immersed in bulk solutions (**Figure 10**). The clay structure is terminated in (010) surfaces, which serve as an interface for exchange of cations and water molecules between the interlayer and the surrounding bulk solution. The resulting broken bonds were saturated by OH and H_2O groups. The two layers were continuous through periodic boundary conditions along the terminated edges. Water molecules were initially randomly distributed in the simulation cell around the centered clay structure. The charge balancing Na^+ or Ca^{2+}ions were divided equally between each basal surface. Energy minimization was performed, followed by an equilibration simulation of 1 ns with the fixed clay structure in the NPT ensemble at 1 bar and 300 K. Actual swelling pressure simulations were then performed as a continuation in the NVT ensemble. The last 40 ns of the total simulation time of 50 ns were used for analysis.

As an unsubstituted reference for the swelling smectites, the work described in section 4.3 investigates the simulated swelling pressure of pyrophyllite. In section 4.4, the model is applied to a series of the montmorillonite-beidellite smectites that vary in layer charge, and charge location (**Table 2**). The investigated smectite structures are shown in **Figure 11**. In section 4.5, the simulation is also extended to the swelling pressure in different salt solutions.

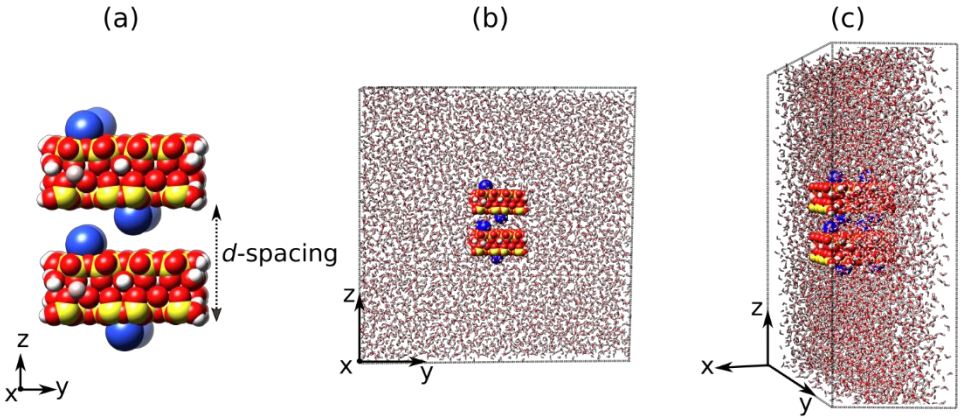

Figure 10. The simulation system contains two clay layers and a surrounding bulk solution. (a) Shows the two clay layers, (b) and (c) provide two views of the simulation cell. The *d*-spacing of the clay shown in the figure is 1.5 nm.

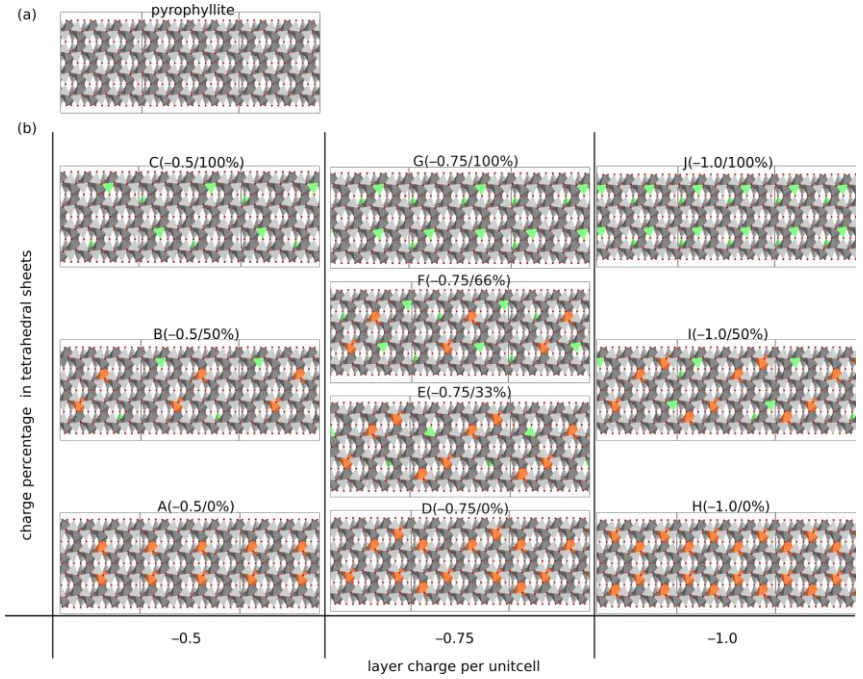

Figure 11. (a) Unsubstituted pyrophyllite reference and (b) substitution arrangements in the studied smectite series. The oxygen atoms are represented by the red spheres. The silica tetrahedrons are colored light grey and the aluminum tetrahedrons are colored green. The alumina octahedrons are colored dark grey and the magnesium octahedrons are colored orange.

Table 2. Total layer charge and charge percentage in T sheets in the studied clay structures.

	Charge (e)		
Structure	per unit cell	per layer	percentage in T sheets
Pyrophyllite	0	0	0
A(–0.5/0%)	–0.5	–4	0
B(–0.5/50%)	–0.5	–4	50
C(–0.5/100%)	–0.5	–4	100
D(–0.75/0%)	–0.75	–6	0
E(–0.75/33%)	–0.75	–6	33
F(–0.75/66%)	–0.75	–6	67
G(–0.75/100%)	–0.75	–6	100
H(–1.0/0%)	–1.0	–8	0
I(–1.0/50%)	–1.0	–8	50
J(–1.0/100%)	–1.0	–8	100

4.3 Model application for pyrophyllite

The swelling pressure modeling was first performed for pyrophyllite, which is known for its non-swelling behaviour. For all simulation starting from structures of 1.0 and 1.2 nm *d*-spacings, a completely dry clay with no interlayer water was achieved in the equilibration state (*d*-spacing at 0.96 nm). All interlayer water molecules were found to move from the interlayer space to the bulk water in the clay surroundings. With further investigations, we found that if two layers of pyrophyllite are separated by a *d*-spacing that is less than 1.4 nm, the clays return to dry condition in the equilibration state. However, if two pyrophyllite layers are separated by over 1.4 nm from each other, they can no longer expel the interlayer water molecules and are able to swell.

It has been noted that the swelling or shrinking of clay depends on the balance of the attraction and repulsion forces acting on two neighbouring smectite layers. For the closely packed pyrophyllite layers, van der Waals attraction is the dominant force; the force is strong enough to expel interlayer water and to bring the two layers of pyrophyllite together. However, when the two layers are more distanced, the van der Waals attraction between two layers is weaker and less capable of expelling the rather large amount of interlayer water molecules. As the van der Waals attractive force decreases, the Brownian motion becomes the dominant force. This is caused by water molecules constantly colliding with the smectite surfaces. Each collision transfers kinetic energy from the water molecule to the layers of smectites and vice versa. If the collision on the two basal surfaces of an individual smectite layer is unbalanced momentarily, the smectites will have net movement in one direction and cause swelling or deswelling. Brownian motion is naturally random thermal motion, however, in the

cases of our model setups, the flexible layer is also more likely to move away from its neighbouring layer that is fixed. The observed swelling behaviour of pyrophyllite with *d*-spacings over 1.4 nm is driven by Brownian motion. In nature, pyrophyllite does not swell to such *d*-spacings; hence there is no chance that Brownian motion would cause any swelling of natural pyrophyllite samples.

The Brownian swelling is depicted in **Figure 12**, with each point representing an independent simulation using a combination of different initial *d*-spacing and spring constant. The descending trend of the swelling pressure as a function of *d*-spacings is observed. Such a descending trend is caused by the nature of the Brownian motion, which drives the individual layers to diffuse away from a zone of relatively high concentration and towards a zone of relatively low concentration of other layers. For non-swelling clays, such as pyrophyllite, the Brownian driven swelling could already be dominant at small *d*-spacings. For swelling clays, the Brownian swelling is significant only for dilute clay suspensions (i.e. at larger *d*-spacings). The van der Waals and ion hydration forces are expected to have more dominant roles at smaller *d*-spacings. In our model setup where two clay layers are immersed in bulk water, the clay layers seems more susceptible to the Brownian motions due to the high edge to surface ratio in our model setups.

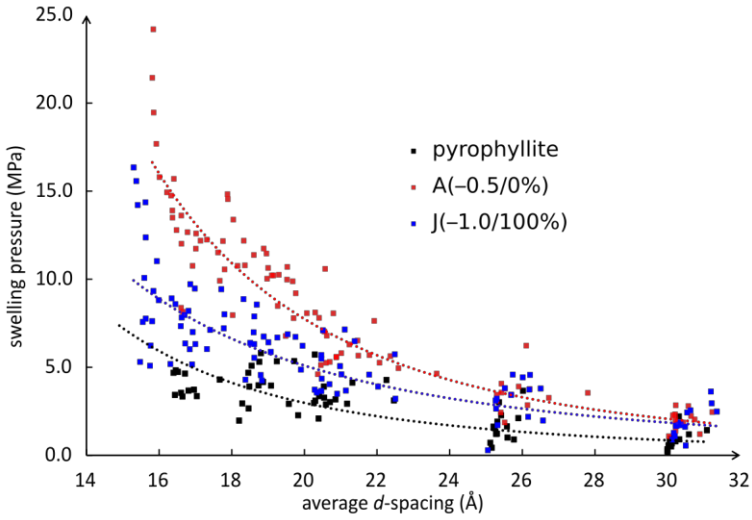

Figure 12. Simulated swelling pressure as a function of average *d*-spacing for pyrophyllite, low charge montmorillonite A(–0.5/0%) and high charge beidellite J(–1.0/100%).

4.4 Model application for montmorillonite-beidellite smectites with various layer charges and charge locations

To account for the influence of layer charge and charge location on the swelling pressure of Na-smectites, the swelling pressure for ten Na-smectite structures with a layer charge ranging from –0.5 to –1.0e per unit cell and a charge location from 0 to 100% in the T sheets is simulated (**Table 2**).

The simulated swelling pressure for two Na-smectite structures having a contrasting layer charge and charge location also demonstrates that swelling pressure declines quickly with increasing *d*-spacings, but is significantly higher than in pyrophyllite (**Figure 12**). Their higher swelling pressure is caused by the interlayer Na^+ ions, which attract water molecules to move from the bulk solution to the interlayer region and subsequently cause the swelling of clays. The initial driving force for swelling at the investigated ranges of *d*-spacings is hence attributed to the forces caused by ion hydration. With strong negative charges in T sheets, J(–1.0/100%) leads to much lower swelling pressure than that of A(–0.5/0%). These results demonstrate that the layer charge and the charge location jointly influence the swelling behaviour of smectite clays. To visualize the swelling behavior of Na-smectites, the swelling pressure at specific *d*-spacings, corresponding to 50%, 100% and 150% expansion states, are plotted in three-dimensional swelling pressure maps in **Figure 13**.

In Na-smectites, the swelling pressure is found to be lower in structures with a higher layer charge from –0.5 to –1.0e per unit cell, regardless of the charge locations. This trend is enhanced by the increase in the charge percentage in T sheets. On the other hand, the swelling pressure is also found to be lower in structures with a higher charge percentage in T sheets, regardless of the layer charge, only that the descending trend is more evident in the case of a high layer charge. Overall, it is evident that the swelling pressure at 50% expansion shows inverse correlation on both the layer charge ranging from –0.5 to –1.0e per unit cell and the charge percentage in T sheets. Such correlation remains significant in the 100% expansion state, but less evident in the 150% expansion states. Hence, these simulation results imply that the influence of layer charge and charge location on the swelling pressure is significant when the smectite structure is compact, while in the swollen structures the influence is less significant. The results give an overall picture of the structural effects on the swelling pressure in the montmorillonite-beidellite series.

The swelling pressure of Ca-smectites with the same layer charge and charge location variables is also simulated. The simulated swelling pressure is found to decrease rapidly as the *d*-spacing increases (**Figure 14**). There is practically no swelling pressure at *d*-spacings over 2.0 nm, which is the upper limit of the 3W of smectites. This is consistent with experimental findings that Ca-smectites do not swell beyond the 3W.[30,54,80]

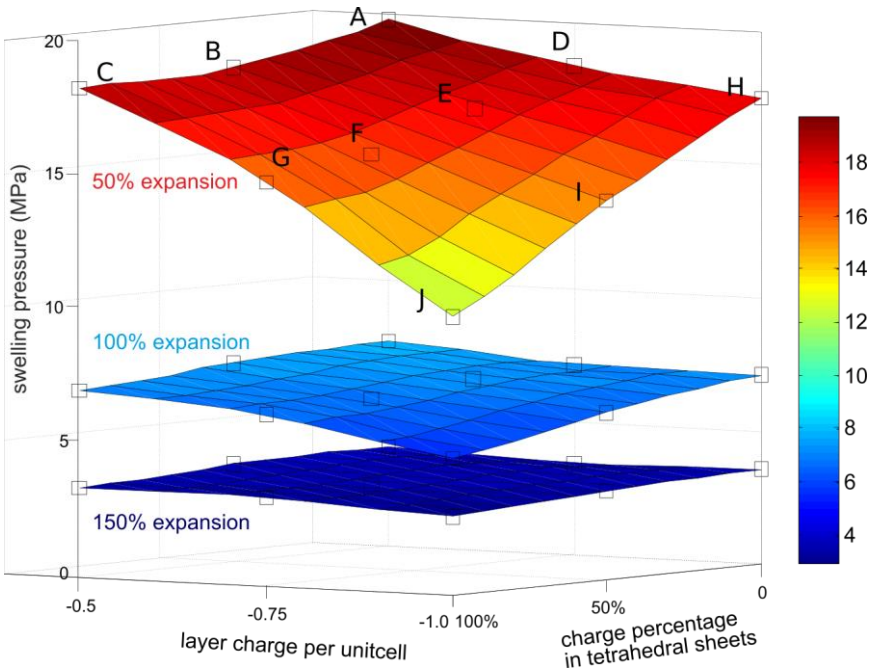

Figure 13. Swelling pressure as a function of layer charge and charge percentage in T sheets. Labels A-J represent the modeled smectites as given in Table 2. The labels also apply to the data for the 100% and 150% expansions.

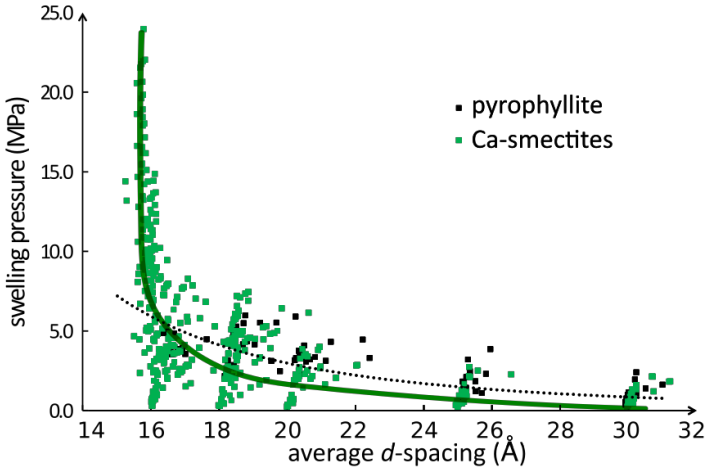

Figure 14. Swelling pressure of Ca-smectites as a function of average *d*-spacing. The green line shows the general trend of the swelling pressures for ten different Ca-smectites.

4.5 Model application for montmorillonites in salt solutions

Montmorillonite A(–0.5/0%) with a layer charge of –0.5e per unit cell is chosen as a representative structure to simulate the influence of saline solutions on the swelling pressure of montmorillonite-beidellite smectite series. The simulated swelling pressure 0.25M sodium chloride (NaCl) and 0.25M calcium chloride ($CaCl_2$) solutions are found to decay exponentially with increasing *d*-spacings (**Figure 15**). Compared to pure water, the clay immersed in salt solutions achieves lower swelling pressure. This could be explained by the differences of water potential in the different environments. Water moves from high to low water potential; and the greater the water potential gradient is, the stronger the swelling is. In the investigated salt solutions, the water potential gradient between the bulk solution and the interlayer was smaller than that in pure water. The larger the gradient between the interlayer and the surrounding solutions, the stronger was the tendency for water to move to dilute the high salt concentrations.

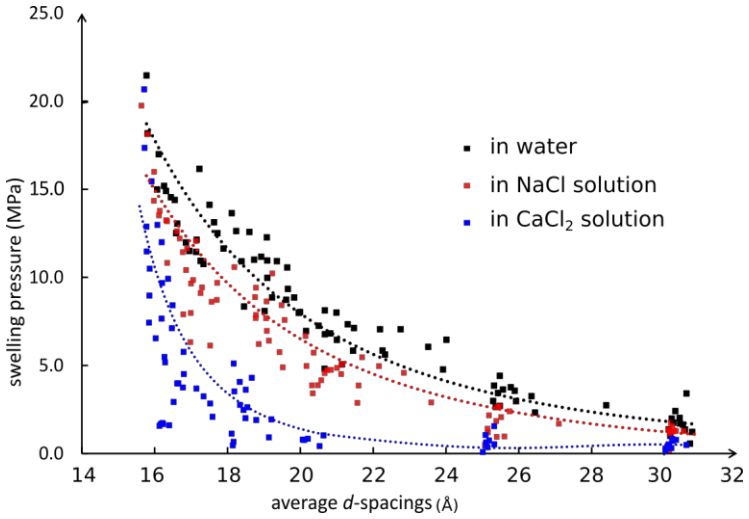

Figure 15. Swelling pressure of Na-montmorillonite in salt solution.

Compared to the swelling pressure in the NaCl solution, the swelling pressure in the $CaCl_2$ solution is significantly lower. By inspecting the dynamic process of simulations, we found that the interlayer Na^+ are gradually exchanged for the Ca^{2+} from the bulk solution. At the equilibrium state, the dominant cations in the interlayer region are thus Ca^{2+} ions. Such an ion exchange process is also supported by experimental observations.[81,82] By transforming from Na-montmorillonite to Ca-montmorillonite, the potential to swell is largely reduced, as reflected in the lower swelling pressures. This also agrees well with the simulation results of Ca-smectites (**Figure 14**).

5 Conclusions

The swelling characteristics and the swelling pressure as influenced by structural and environmental variables are the main focus of this study. The swelling curve of a montmorillonite clay structure and its interlayer structure were investigated with the emphasis being on the water content and interlayer cation compositions. Regardless of the interlayer cation composition, non-linear increase in *d*-spacing was observed with increasing water content. However, the larger hydration energy of Ca^{2+} ions relative to Na^{+} ions causes higher water coordination numbers and more pronounced association of water molecules with Ca^{2+} ions. Since Ca^{2+} prefers to be fully coordinated to water molecules, the 2-layer hydrate readily forms at rather lower water contents. The layer hydrates are stable in relation to changes in temperature and pressure compared to other mixed layer hydrates.

An approach to predict swelling pressure of swelling clays was proposed and justified, using a clay-water system. The molecular dynamics simulations demonstrate that experimentally determined general swelling trends of Na-montmorillonite in pure water can be reproduced with good accuracy. The approach was further applied to a study of the influence of smectite structural factors. A systematic analysis of swelling pressures of Na- and Ca-smectites with varying layer charge and charge location was performed. The simulation suggested that the swelling pressure is inversely correlated to both layer charge ranging from –0.5 to –1.0e per unit cell and the charge percentage in T sheets. Such influences are evident in compacted clays, but become less significant in delaminated smectites. Ca-smectites were found to be non-swelling beyond 3-layer hydrate. The results are in a good agreement with the experimental findings. Furthermore, the approach was utilized to examine the effect of saline solutions. Swelling pressures showed a marked decrease as the bulk solution changes from water to saline solutions including NaCl and $CaCl_2$ solutions.

The study reported herein introduced and justified a new concept for simulating the swelling clay-water systems with particular emphasis on the swelling behavior and swelling pressure. Structural factors in the montmorillonite-beidellite series may be now systematically taken into account when studying the influence of layer charge and charge location on the swelling pressure of dioctahedral smectites. Overall, the new approach can be extended to other clay systems and is expected to be useful in the prediction and comparison of the swelling behavior and swelling pressure of swelling clays in the context of HLRW geological disposal and other industrial applications.

Acknowledgements

This research was carried out at the Department of Chemistry, University of Eastern Finland during the years 2012–2015. The work was funded by the Finnish Agency for Technology and Innovation TEKES and the European Union/European Regional Development Fund ERDF (LP project, 2012-2014) and Posiva Oy (MMT swelling pressure and TOT charge distribution, 2015). The Department of Chemistry provided a grant for finalizing the thesis. The computations were supported by Finnish Grid Infrastructure resources.

I would like to express my deep gratitude to my supervisor, Prof. Tapani Pakkanen for his guidance, commitment and enormous support throughout the years. Dr. Janne Hirvi is gratefully acknowledged for his solid contribution to the research planning, implementation and article writing. Dr. Jukka Tanskanen is thanked for introducing me to the world of clay sciences and all the help with article I.

It was an honor for me to work in close collaboration with teams from Posiva Oy and B+Tech Oy. I want to thank Kari Koskinen, Seppo Kasa, Timothy Schatz, Rasmus Eriksson and Teemu Laurila for productive collaboration. My special acknowledgements go to Seppo Kasa for his continuous support to the research, and Timothy Schatz for his critical comments and language corrections on articles I and II.

I would like to give my thanks to the staffs of the chemistry department for their care and kind help. I had a pleasant time working with Chian Ye Ling. Lasse Lavikainen is also thanked for cooperation. Mari Heiskanen, Sari Suvanto, and Eija Faari-Kapanen are thanked for taking care many of my practical issues/questions with great patience. My dearest thanks goes to Shi-Yun Wu for sharing the ups and downs, good and bad times with me. The warmest gratitude also goes to Adil, Minh, Gomathy, Senthil, Katinka, Wenjuan, Yuanyuan, Qing, Ming and Aifang for all their support and accompany.

I would like to dedicate this thesis to my grandma in heaven, Shucai Yang. I am grateful to my parents (Yuequn Sun and Qingfen Meng) and my dear lovely sisters (Jinwei Sun, Xinzhu Sun and Tingting Sun) for their unconditional love. I am also thankful to have Yufu Zhao and Shuming Gong as the best parents-in-law. Uncle Yanfei Yang is thanked for his care and love. I would like to express my sincere gratitude to Heli Peltola and Seppo Kellomäki for being my “Finnish families” and taking care of me. My sincere appreciation is extended to Kaiyun Wang for being a great mentor over the years. Finally, I would like to thank my husband, Jinnan Gong, for his love and support. You are the best thing that ever happened to me. Love you.

References

(1) Bergaya, F.; Lagaly, G. *Handbook of Clay Science* **2013**, 3–7.

(2) Murray, H. H. Applied Clay Mineralogy Today and Tomorrow. *Clay Miner* **1999**, *34* (1), 39–39.

(3) Odom, I. E. Smectite Clay Minerals: Properties and Uses. *Phil. Trans. R. Soc. Lond. A* **1984**, 311, 391–409.

(4) Grim, R. E.; Guven, N. Bentonites – Geology, Mineralogy, Properties and Use. *Developments in Sedimentology* **1979**, *24* (3-4), 324–325.

(5) Alther, G. R. The Qualifications of Bentonite as a Soil Sealant. *Eng. Geol.* **1987**, *23* (3-4), 177–191.

(6) de Pablo, L.; Chávez, M. L.; Abatal, M. Adsorption of Heavy Metals in Acid to Alkaline Environments by Montmorillonite and Ca-Montmorillonite. *Chem. Eng. J.* **2011**, *171* (3), 1276–1286.

(7) Van Gunsteren, W. F.; Berendsen, H. J. C. Computer Simulation of Molecular Dynamics: Methodology, Applications, and Perspectives in Chemistry. *Angew.Chem.Int.Ed.Engl* **1990**, *29* (9), 992–1023.

(8) Talukdar, D.; Das, G.; Thakur, S.; Karak, N.; Thakur, A. J. Copper Nanoparticle Decorated Organically Modified Montmorillonite (OMMT): an Efficient Catalyst for the N-Arylation of Indoles and Similar Heterocycles. *Catal. Commun.* **2015**, *59*, 238–243.

(9) Kloprogge, J. T. Synthesis of Smectites and Porous Pillared Clay Catalysts: a Review. *J. Porous Mater.* **1998**, *5* (1), 5–41.

(10) Breen, C.; Moronta, A. Characterization and Catalytic Activity of Aluminum- and Aluminum/Tetramethylammonium-Exchanged Bentonites. *J. Phys. Chem. B* **2000**, *104* (12), 2702–2708.

(11) Ravindra Reddy, C.; Nagendrappa, G.; Jai Prakash, B. S. Surface Acidity Study of Mn+-Montmorillonite Clay Catalysts by FT-IR Spectroscopy: Correlation with Esterification Activity. *Catal. Commun.* **2007**, *8* (3), 241–246.

(12) Guo. J.; Al-Dahhan, M. Catalytic Wet Oxidation of Phenol by Hydrogen Peroxide Over Pillared Clay Catalyst. *Ind. Eng. Chem. Res.* **2003**, *42* (12), 2450–2460.

(13) Occelli, M. Cracking Selectivity of a Delaminated Clay Catalyst. *J. Catal.*

1984, *90* (2), 256–260.

(14) Varma, R. S. Clay and Clay-Supported Reagents in Organic Synthesis. *Tetrahedron* **2002**, *58* (7), 1235–1255.

(15) Jaynes, W.; Zartman, R.; Hudnall, W. Aflatoxin B1 Adsorption by Clays from Water and Corn Meal. *Appl. Clay Sci* **2007**, *36* (1-3), 197–205.

(16) Carretero, M. I.; Pozo, M. Clay and Non-Clay Minerals in the Pharmaceutical Industry. *Appl. Clay Sci* **2009**, *46* (1), 73–80.

(17) Mittal, V. Polymer Layered Silicate Nanocomposites: a Review. *Materials*. 2009, *2* (3), 992–1057.

(18) Higgo, J. Clay as a Barrier to Radionuclide Migration. *Prog. Nucl. Energy* **1987**, *19* (2), 173–207.

(19) Pusch, R. Use of Bentonite for Isolation of Radioactive Waste Products. *Clay Miner* **1992**, *27*, 353–361.

(20) Heidin A. Long-Term Safety for the Final Repository for Spent Nuclear Fuel at Forsmark - Main Report of the SR-Site Project, Volume I. TR-reports 11-01 **2011**.

(21) Posiva Oy website. http://www.posiva.fi/en/final_disposal/basics_of_the_final_disposal (accessed 12/30, 2015)

(22) Karnland, O.; Olsson, S.; Nilsson, U. Mineralogy and Sealing Properties of Various Bentonites and Smectite-Rich Clay Materials. *SKB TR-06-30* **2006**.

(23) Emmerich, K.; Wolters, F.; Kahr, G.; Lagaly, G. Clay Profiling: the Classification of Montmorillonites. *Clays Clay Miner* **2009**, *57* (1), 104–114.

(24) Pusch, R. The Buffer and Backfill Handbook. Part 2: Materials and Techniques. *SKB TR-02-12* **2002**.

(25) Slade, P. G.; Quirk, J. P.; Norrish, K. Crystalline Swelling of Smectite Samples in Concentrated NaCl Solutions in Relation to Layer Charge. *Clays Clay Miner* **1991**, *39*, 234–238.

(26) Greathouse, J.; Sposito, G. Monte Carlo and Molecular Dynamics Studies of Interlayer Structure in Li(H_2O) 3−Smectites. *J. Phys. Chem. B* **1998**, *102* (13), 2406–2414.

(27) Liu, X.; Lu, X.; Wang, R.; Zhou, H. Effects of Layer-Charge Distribution on

the Thermodynamic and Microscopic Properties of Cs-Smectite. *Geochim. Cosmochim. Acta.* **2008**, *72* (7), 1837–1847.

(28) Boek, E. S.; Coveney, P. V.; Skipper, N. T. Molecular Modeling of Clay Hydration: a Study of Hysteresis Loops in the Swelling Curves of Sodium Montmorillonites. *Langmuir* **1995**, *11* (12), 4629–4631.

(29) Segad, M.; Åkesson, T.; Cabane, B.; Jönsson, B. Nature of Flocculation and Tactoid Formation in Montmorillonite: the Role of pH. *Phys. Chem. Chem. Phys.* **2015**.

(30) Norrish, K. The Swelling of Montmorillonite. *Discuss. Faraday Soc.* **1954**, *18* (0), 120–134.

(31) Young, D. A.; Smith, D. E. Simulations of Clay Mineral Swelling and Hydration: Dependence upon Interlayer Ion Size and Charge. *J. Phys. Chem. B* **2000**, *104* (39), 9163–9170.

(32) Laird, D. A. Layer Charge Influences on the Hydration of Expandable 2: 1 Phyllosilicates. *Clays Clay Miner* **1999**, 47(5)630-636.

(33) Smith, D. E.; Wang, Y.; Chaturvedi, A.; Whitley, H. D. Molecular Simulations of the Pressure, Temperature, and Chemical Potential Dependencies of Clay Swelling †. *J. Phys. Chem. B* **2006**, *110* (40), 20046–20054.

(34) Sato, T.; Watanabe, T.; Otsuka, R. Effects of Layer Charge, Charge Location, and Energy Change on Expansion Properties of Dioctahedral Smectites. *Clays Clay Miner.* **1992**.

(35) Laird, D. A. Influence of Layer Charge on Swelling of Smectites. *Appl. Clay Sci* **2006**, *34* (1-4), 74–87.

(36) Zhang, F.; Zhang, Z. Z.; Low, P. F.; Roth, C. B. The Effect of Temperature on the Swelling of Montmorillonite. *Clay Miner.* **1993**, *28*, 25–31.

(37) Villar, M. V.; Lloret, A. Influence of Temperature on the Hydro-Mechanical Behaviour of a Compacted Bentonite. *Appl. Clay Sci.* **2004**, *26* (1-4), 337–350.

(38) Mooney, R.; Keenan, A.; Wood, L. Adsorption of water vapor by montmorillonite. II. Effect of exchangeable ions and lattice swelling as measured by X-ray diffraction. *J. Am. Chem. Soc.* **1952**, *74*, 1371-1374.

(39) Bérend, I.; Cases, JM.; Frangois, M.; Uriot, JP.; Michot, L.; Masion, A., Thomas, E. Mechanism of adsorption and desorption of water vapor by homoionic montmorillonites : 2. The Li^+, Na^+, K^+, Rb^+ and the Cs^+ exchanged

form. *Clays Clay Miner*. **1995**, 43, 324-336.

(40) Karaborni, S.; Smit, B.; Heidug, W.; Urai, J.; Van Oort, E. The Swelling of Clays: Molecular Simulations of the Hydration of Montmorillonite. *Science* **1996**, *271*, 1102–1104.

(41) De Pablo-Galan, L.; Chavez-Garcia, M. L. Simulation of the Stability of Na-, K-, and Ca-Montmorillonite at High Temperatures and Pressures. *Geochim. Cosmochim. Acta*. **2006**, *70* (18), A466-A510.

(42) Christidis, G. E.; Blum, A. E.; Eberl, D. D. Influence of Layer Charge and Charge Distribution of Smectites on the Flow Behaviour and Swelling of Bentonites. *Appl. Clay Sci*. **2006**, *34* (1-4), 125–138.

(43) Chiou, C. T.; Rutherford, D. W. Effects of Exchanged Cation and Layer Charge on the Sorption of Water and EGME Vapors on Montmorillonite Clays. *Clays Clay Miner*. **1997**, *45* (6), 867–880.

(44) Michot, L. J. Hydration and Swelling of Synthetic Na-Saponites: Influence of Layer Charge. *Am. Mineral*. **2005**, *90* (1), 166–172.

(45) Anderson, R. L.; Ratcliffe, I.; Greenwell, H. C.; Williams, P. A.; Cliffe, S.; Coveney, P. V. Clay Swelling — a Challenge in the Oilfield. *Earth-Sci. Rev*. **2010**, *98* (3-4), 201–216.

(46) Teich-McGoldrick, S. L.; Greathouse, J. A.; Jové-Colón, C. F.; Cygan, R. T. Swelling Properties of Montmorillonite and Beidellite Clay Minerals From Molecular Simulation: Comparison of Temperature, Interlayer Cation, and Charge Location Effects. *J. Phys. Chem. C* **2015**, *119* (36), 20880–20891.

(47) Tambach, T. J.; Hensen, E. J. M.; Smit, B. Molecular Simulations of Swelling Clay Minerals. *J. Phys. Chem. B* **2004**, *108* (23), 7586–7596.

(48) Hensen, E. J. M.; Smit, B. Why Clays Swell. *J. Phys. Chem. B* **2002**, *106* (49), 12664–12667.

(49) Karnland, O. Bentonite Swelling Pressure in Strong NaCl Solutions. Correlation between Model Calculations and Experimentally Determined Data. *POSIVA 98-01* **1998**.

(50) Sun, W-J.; Wei, Z-F.; Sun, D-A.; Liu, S-Q.; Fatahi, B.; Wang, X-Q. Evaluation of the Swelling Characteristics of Bentonite–Sand Mixtures. *Eng. Geol*. **2015**, *199*, 1–11.

(51) Karnland, O. Chemical and Mineralogical Characterization of the Bentonite Buffer for the Acceptance Control Procedure in a KBS-3 Repository. *Swedish*

Nuclear Fuel and Waste Management Co., Stockholm (Sweden), **2010**.

(52) Wang, Q.; Tang, A. M.; Cui, Y.-J.; Delage, P.; Gatmiri, B. Experimental Study on the Swelling Behaviour of Bentonite/Claystone Mixture. *Eng. Geol.* **2012**, *124*, 59–66.

(53) Kaufhold, S.; Baille, W.; Schanz, T.; Dohrmann, R. About Differences of Swelling Pressure—Dry Density Relations of Compacted Bentonites. *Appl. Clay Sci.* **2015**, *107*, 52–61.

(54) Lee, J. O.; Lim, J. G.; Mo Kang, Il; Kwon, S. Swelling Pressures of Compacted Ca-Bentonite. *Eng. Geol.* **2012**, *129-130* (C), 20–26.

(55) Cygan, R. T.; Greathouse, J. A.; Heinz, H.; Kalinichev, A. G. Molecular Models and Simulations of Layered Materials. *J. Mater. Chem.* **2009**, *19* (17), 2470–2481.

(56) Hess, B.; Kutzner, C.; van der Spoel, D.; Lindahl, E. GROMACS 4: Algorithms for Highly Efficient, Load-Balanced, and Scalable Molecular Simulation. *J. Chem. Theory Comput.* **2008**, *4* (3), 435–447.

(57) Cygan, R. T.; Liang, J.-J.; Kalinichev, A. G. Molecular Models of Hydroxide, Oxyhydroxide, and Clay Phases and the Development of a General Force Field. *J. Phys. Chem. B* **2004**, *108* (4), 1255–1266.

(58) Cygan, R. T.; Greathouse, J. A.; Heinz, H.; Kalinichev, A. G. Molecular Models and Simulations of Layered Materials. *J. Mater. Chem.* **2009**, *19* (17), 2470–2481.

(59) Teleman, O.; Jönsson, B.; Engström, S. A Molecular Dynamics Simulation of a Water Model with Intramolecular Degrees of Freedom. *Mol. Phys.* **2006**, *60* (1), 193–203.

(60) Skipper, N. T.; Sposito, G.; Chang, F. Monte Carlo Simulation of Interlayer Molecular Structure in Swelling Clay Minerals. 2. Monolayer Hydrates. *Clays Clay Miner.* **1995**, *43*, 294–303.

(61) Emmerich, K.; Koeniger, F.; Kaden, H.; Thissen, P. Microscopic Structure and Properties of Discrete Water Layer in Na-Exchanged Montmorillonite. *J.Colloid Interface Sci.* **2015**, *448*, 24–31.

(62) Karnland, O.; Olsson, S.; Nilsson, U. Mineralogy and Sealing Properties of Various Bentonites and Smectite-Rich Clay Materials. *SKB TR-06-30* **2006**.

(63) Boek, E. S.; Coveney, P. V.; Skipper, N. T. Monte Carlo Molecular Modeling Studies of Hydrated Li-, Na-, and K-Smectites: Understanding the Role of

Potassium as a Clay Swelling Inhibitor. *J*. *Am*. *Chem*. *Soc*. **1995**, *117* (50), 12608–12617.

(64) Fu, M. H.; Zhang, Z. Z.; Low, P. F. Changes in the Properties of a Montmorillonite-Water System during the Adsorption and Desorption of Water: Hysteresis. *Clays Clay Miner*. **1990**, *38*, 485–492.

(65) Zheng, Y.; Zaoui, A.; Shahrour, I. A Theoretical Study of Swelling and Shrinking of Hydrated Wyoming Montmorillonite. *Appl*. *Clay Sci*. **2011**, *51* (1-2), 177–181.

(66) Keren, R.; Shainberg, I. Water Vapor Isotherms and Heat of Immersion of Na/Ca-Montmorillonite Systems-I: Homoionic Clay. *Clays Clay Miner*. **1975**.

(67) Cases, J. M.; Bérend, I.; François, M.; Uriot, J. P. Mechanism of Adsorption and Desorption of Water Vapor by Homoionic Montmorillonite; 3, the Mg^{2+}, Ca^{2+}, and Ba^{3+} Exchanged Forms. *Clays Clay Miner*. **1997**, *45*, 8–22.

(68) Bray, H. J.; Redfern, S. Influence of Counterion Species on the Dehydroxylation of Ca^{2+}-, Mg^{2+}-, Na^{+}-And K^{+}-Exchanged Wyoming Montmorillonite. *Mineral*. *Mag*. **2000**, 64(2), 337-346.

(69) Bray, H. J.; Redfern, S. A. T.; Clark, S. M. The Kinetics of Dehydration in Ca-Montmorillonite; an in Situ X-Ray Diffraction Study. *Mineral*. *Mag*. **1998**, *62* (5), 647–656.

(70) Anderson, M. A.; Trouw, F. R.; Tam, C. N. Properties of Water in Calcium- and Hexadecyltrimethylammonium-Exchanged Bentonite. *Clays Clay Miner*. **1999**.

(71) Cebula, D.; Thomas, R.; Middleton, S.; Ottewill, R.; White, J. Neutron diffraction from clay-water systems. *Clays Clay Miner*. **1979**, *27*, 39-52.

(72) Hawkins, R.; Egelstaff, P. Interfacial water structure in montmorillonite from neutron diffraction experiments. *Clays Clay Miner*. **1980**, 28(1), 19-28.

(73) Kraehenbuehl, F.; Stoeckli, H. F.; Brunner, F.; Kahr, G.; Mueller-Vonmoos, M. Study of the Water-Bentonite System by Vapour Adsorption, Immersion Calorimetry and X-Ray Techniques: I. Micropore Volumes and Internal Surface Areas, Following Dubinin's Theory. *Clay Miner*. **1987**, *22*, 1–9.

(74) Cases, J. M.; Bérend, I.; Besson, G.; François, M.; Uriot, J. P. Mechanism of Adsorption and Desorption of Water Vapor by Homoionic Montmorillonite. 1. the Sodium-Exchanged Form. *Langmuir* **1992**, *8* (11), 2730–2739.

(75) Porion, P.; Michot, L.; Faugère, A. M.; Delville, A. Structural and Dynamical

Properties of the Water Molecules Confined in Dense Clay Sediments: a Study Combining ^{2}H NMR Spectroscopy and Multiscale Numerical Modeling. *J*. *Phys*. *Chem*. *C* **2007**, *111* (14), 5441–5453.

(76) Ormerod, E.; Newman, A. Water sorption on Ca-saturated clays: II. Internal and external surfaces of montmorillonite. *Clay Miner*. **1983**, *18*, 289-299.

(77) Bray, H. J.; Redfern, S. A. T. Kinetics of Dehydration of Ca-Montmorillonite. *Phys Chem Miner*. **1999**, *26* (7), 591–600.

(78) Cui, Y-J.; Yahia-Aissa, M.; Delage, P. A Model for the Volume Change Behavior of Heavily Compacted Swelling Clays. *Eng*. *Geol*. **2002**, *64*, 233–250.

(79) Sun, D.; Cui, H.; Sun, W. Swelling of Compacted Sand–Bentonite Mixtures. *Appl*. *Clay Sci*. **2009**, *43* (3-4), 485–492.

(80) Segad, M.; Jönsson, B.; Åkesson, T.; Cabane, B. Ca/Na Montmorillonite: Structure, Forces and Swelling Properties. *Langmuir* **2010**, *26* (8), 5782–5790.

(81) Herbert, H. J.; Moog, H. C. Cation Exchange, Interlayer Spacing, and Water Content of MX-80 Bentonite in High Molar Saline Solutions. *Eng*. *Geol*. **1999**, *54* (1-2), 55–65.

(82) Li, Y.; Wang, X.; Wang, J. Cation Exchange, Interlayer Spacing, and Thermal Analysis of Na/Ca-Montmorillonite Modified with Alkaline and Alkaline Earth Metal Ions. *J Therm Anal Calorim*. **2011**, *110* (3), 1199–1206.

106/2011 RÖNKKÖ Hanna-Leena: Studies on $MgCl_2$/alcohol adducts and a self-supported Ziegler-Natta catalyst for propene polymerization

107/2011 KASANEN Jussi: Photocatalytic TiO_2-based multilayer coating on polymer substrate for use in self-cleaning applications

108/2011 KALLIO Juha: Structural studies of *Ascomycete* laccases – Insights into the reaction pathways

109/2011 KINNUNEN Niko: Methane combustion activity of Al_2O_3-supported Pd, Pt, and Pd-Pt catalysts: Experimental and theoretical studies

110/2011 TORVINEN Mika: Mass spectrometric studies of host-guest complexes of glucosylcalixarenes

111/2012 KONTKANEN Maija-Liisa: Catalyst carrier studies for 1-hexene hydroformulation: cross-linked poly(4-vinylpyridine), nano zinc oxide and one-dimensional ruthenium polymer

112/2012 KORHONEN Tuulia: The wettability properties of nano- and micromodified paint surfaces

113/2012 JOKI-KORPELA Fatima: Functional polyurethane-based films and coatings

114/2012 LAURILA Elina: Non-covalent interactions in Rh, Ru, Os, and Ag complexes

115/2012 MAKSIMAINEN Mirko: Structural studies of *Trichoderma reesei, Aspergillus oryzae* and *Bacillus circulans* sp. *alkalophilus* beta-galactosidases – Novel insights into a structure-function relationship

116/2012 PÖLLÄNEN Maija: Morphological, thermal, mechanical, and tribological studies of polyethylene composites reinforced with micro– and nanofillers

117/2013 LAINE Anniina: Elementary reactions in metallocene/methylaluminoxane catalyzed polyolefin synthesis

118/2013 TIMONEN Juri: Synthesis, characterization and anti-inflammatory effects of substituted coumarin derivatives

119/2013 TAKKUNEN Laura: Three-dimensional roughness analysis for multiscale textured surfaces: Quantitative characterization and simulation of micro- and nanoscale structures

120/2014 STENBERG Henna: Studies of self-organizing layered coatings

121/2014 KEKÄLÄINEN Timo: Characterization of petroleum and bio-oil samples by ultrahigh-resolution Fourier transform ion cyclotron resonance mass spectrometry

122/2014 BAZHENOV Andrey: Towards deeper atomic-level understanding of the structure of magnesium dichloride and its performance as a support in the Ziegler-Natta catalytic system

123/2014 PIRINEN Sami: Studies on $MgCl_2$/ether supports in Ziegler–Natta catalysts for ethylene polymerization

124/2014 KORPELA Tarmo: Friction and wear of micro-structured polymer surfaces

125/2014 HUOVINEN Eero: Fabrication of hierarchically structured polymer surfaces

126/2014 EROLA Markus: Synthesis of colloidal gold and polymer particles and use of the particles in preparation of hierarchical structures with self-assembly

127/2015 KOSKINEN Laura: Structural and computational studies on the coordinative nature of halogen bonding

128/2015 TUIKKA Matti: Crystal engineering studies of barium bisphosphonates, iodine bridged ruthenium complexes, and copper chlorides

129/2015 JIANG Yu: Modification and applications of micro-structured polymer surfaces

130/2015 TABERMAN Helena: Structure and function of carbohydrate-modifying enzymes

131/2015 KUKLIN Mikhail S.: Towards optimization of metalocene olefin polymerization catalysts via structural modifications: a computational approach

132/2015 SALSTELA Janne: Influence of surface structuring on physical and mechanical properties of polymer-cellulose fiber composites and metal-polymer composite joints

133/2015 CHAUDRI Adil Maqsood: Tribological behavior of the polymers used in drug delivery devices

134/2015 HILLI Yulia: The structure-activity relationship of Pd-Ni three-way catalysts for H_2S suppression